

Exploring the impact of weather variability on bioenergy and variable renewable energy

Sandra Gutjahr*, Danial Esmaeili Aliabadi*, Daniela Thrän*,

*Helmholtz Centre for Environmental Research - UFZ, Permoserstraße 15, 04318 Leipzig, Germany

Corresponding author's email: sandra.gutjahr@ufz.de

Abstract—The energy sector is the biggest contributor to greenhouse gas emissions. The need to decarbonize the energy sector leads to increasing investment in renewable energy sources. While variable renewable energy (VRE) such as wind and solar photovoltaics introduces fluctuations, depending on weather variability, bioenergy – with its inherent flexibility – can mitigate the negative impacts of the intermittency on a net-zero emissions energy system. Furthermore, biomass removes atmospheric carbon dioxide, assisting us to reach climate goals. This work presents the integration of stochasticity into the extended bioenergy optimization model (BENOPTex) to analyze the interplay between VRE and dispatchable bioenergy. The findings demonstrate that for large amounts of solar and wind energy, the overall system cost is at the minimum, whereas during shortages, flexible bioenergy can support meeting electricity demand but at a higher system cost.

Index Terms—Bioenergy, energy optimization models, solar, stochastic models, wind,

I. INTRODUCTION

In order to fulfill the climate targets and stay on track to 1.5 °C, further accelerated investments in the expansion of variable renewable energy (VRE), such as solar and wind power, will be essential [1]. While these renewable technologies are experiencing massive cost reductions and technological development, fossil fuel extraction cost is continuously increasing [2]. In some places, even now, solar PV passed the grid parity point and became the cheapest form of electricity generation [3]; however, VRE depends on meteorological factors (e.g., wind speed, irradiation, temperature). With the further de-fossilization of the energy system, electricity demand will increase, as will the need for flexibility to compensate for the unpredictability of VRE. Considering the techno-economic challenges, direct electrification won't be feasible for some energy-intensive processes [4]; thus, using biomass as a relatively storable energy source (i.e., short-term and mid-term storage) with versatile usage options can be a more cost-effective alternative [5], [6]. Although utility-scale battery energy storage systems (BESS) can reduce emissions, their high storage costs pose significant economic challenges [7].

As an indispensable part of energy supply chain management, energy system optimization models (ESOMs) have been used over the last 50 years to inform decision- and policy-makers about strategic planning and future complexities of the energy system [8], [9]. Initially developed during the oil crises and political conflicts of the 1970s, these models aimed to

assess the impacts of geopolitical instability on energy security and resource allocation. However, as the energy landscape evolved and the global focus shifted towards sustainability, ESOMs have adapted to incorporate the growing importance of VRE [10]. The first generation of ESOMs have ignored VRE's probabilistic nature by exploiting deterministic scenarios to evaluate long-term uncertainties of various narrative storylines [11]. To make matters worse, the lower resolution of these models tends to overestimate the contribution from VRE (i.e., viewing VRE as a silver bullet) and underestimate CO₂ emissions [12]. Also, the coarse representation of variability leads to underestimation of total system cost [13].

Scientists employ multiple approaches to deal with the uncertainty of the system under investigation, such as scenario analysis, sensitivity analysis, and uncertainty analysis [14]. Depending on the research objectives, researchers may utilize scenario analysis to focus on a certain number of plausible futures or use sensitivity analysis to find the magnitude of system responses to variable inputs, or uncertainty analysis when the probabilistic information of these variable inputs is available. Stochastic modeling emerged as a way of representing short-term variability in long-term energy models. Unlike deterministic models, where decisions are based on a single operational scenario with a probability of realization set at 100%, stochastic models define scenarios by considering the likelihood of different outcomes. Therefore, a major stochastic modeling challenge is to quantify various realizations' probability. When quantification is not possible (especially for extreme events), robust optimization can be employed [15]. Robust optimization uses uncertainty sets instead of stochastic scenarios [16]. The technique renders solutions that exhibit feasibility for all possible realizations of uncertainty within a range defined in the uncertainty set. Stochastic and robust modeling improve the representation of VRE in long-term energy models by capturing the need for backup capacity and flexible solutions.

When performing scenario analysis, extremes must also be considered [17]; therefore, to explore the interplay of integrated variability with bioenergy, this paper examines scenarios representing the best possible outcome, the worst possible outcome, and an average outcome. In this study, we investigate the interplay between VRE and dispatchable energy resources, considering historical data. To this end, the uncertain power generation of onshore and offshore wind power and solar PV will be integrated into the extended

bioenergy optimization model of the German energy system [18] via random variables. We combine modeling extremes scenarios with sensitivity analysis to explore the solution space.

II. METHODOLOGY

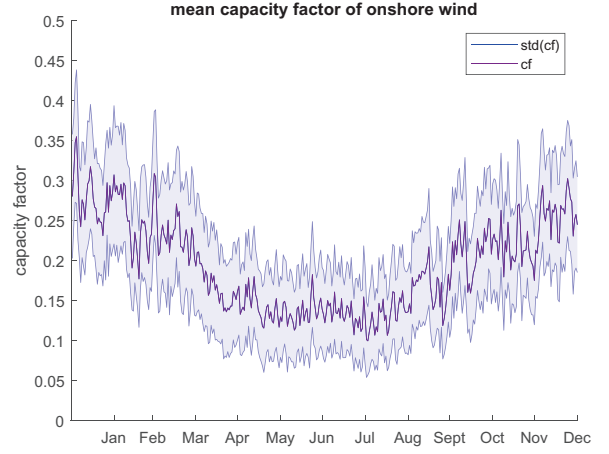
A. Retrieving historical data

To model the intermittencies, we collected capacity factors (cf) for wind (onshore and offshore) and solar PV from Renewables.Ninja [19], [20]. These hourly cfs are the outcomes of simulations based on past weather information from 1980 until 2016 and updated until 2019 on a national scale for all European countries. cf describes the ratio of actual energy generation to the potential energy generation during a given period. Data from the 29th of February was extracted from the dataset. Figure 1 illustrates the variation in cf based on the energy source. Figure 1a shows the mean daily cf for onshore wind in Germany, averaged over 24 hours, from 1980 to 2019. In comparison to the rest of the year, less wind is available during the summer months and a higher variability in February and November is shown. In comparison, Figure 1b shows the median capacity factor for solar PV in Germany averaged over all summer days between 1980 to 2019 with the respective calculated percentiles. The capacity factor is zero at night and reaches its maximum at noon. Not shown is the smaller maximum cf of PV on winter days, while in contrast, the cf of wind reaches its maximum during the winter months. Thus, there is a region-time-dependent complementary relationship between wind and solar.

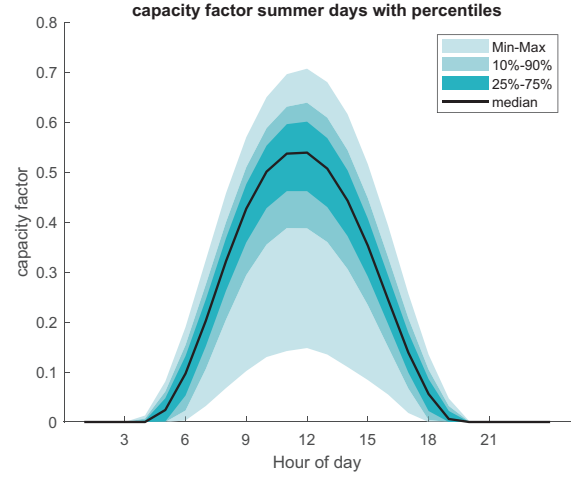
B. Optimization Model

The selected optimization model for this study is *BENOPTex* [21], as it is a technologically and spatially detailed deterministic model that considers the latest policies in place. For instance, the Renewable Energy Directive (RED) is considered according to the base scenario of [22]. Regional hourly electricity demand is harmonized through the coupling of REMix and *BENOPTex* models [23]. The model is limited to Germany with detailed information on the German biomass potential and transmission lines. For this study, the power sector has been expanded, allowing the model to invest in VREs as well as dispatchable technologies. Doing so enables us to introduce historic cf values in the model as various stochastic events that may occur in the future.

Incorporating stochasticity into *BENOPTex* enables the analysis of the impact of variable electricity generation on both the overall system cost and the biomass consumption for energy production. In order to model the intermittency of wind and solar, a stochastic decision variable for each VRE in every time slice of each year is introduced. The time horizon of our model is from 2020 until 2050, with yearly time steps ($t \in T$). However, each year is broken down into time slices ($j \in J$). In the deterministic model, Eq. (1) limits the amount of electricity (E^{el}) that can be produced (in PJ) from a technology i at time slice j of year t in region r , where β_j converts GWh to PJ considering the maximum number of time



(a) Mean capacity factor of wind onshore with standard deviation.



(b) Capacity factor for solar PV from 1980 until 2019 for summer days with percentiles.

Fig. 1: Mean cf of onshore wind averaged per day, and over all years (1a, and mean cf of solar PV for summer days(1b).

slices ($J^{max} = |J|$), k_{ti} is the deployed capacity in GW, and C_{tir} specifies the availability of technology i at year t in region r . C_{tir} excludes the maintenance time when power plants cannot produce electricity. This constraint is mostly active as VREs often do not incur variable operation and maintenance costs.

$$E_{tjir}^{el} \leq \beta_j k_{ti} C_{tir}, \forall i \in I^{\text{CONVel}}, j \in J, r \in R \quad (1)$$

$$\beta_j = \left(\frac{8760 \cdot 0.0036}{J^{max}} \right), \forall j \in J$$

However, the capacity factor of intermittent renewable technologies are random stochastic variables (\tilde{C}_{tir}) that are de-

pendent on weather conditions.

$$E_{tjir}^{el} \leq \beta_j k_{ti} \tilde{C}_{tjir} \quad , \forall i \in I^{VRE}, j \in J, r \in R \quad (2)$$

Different realizations of \tilde{C}_{tjir} in Eq. (2) can be formulated using scenarios. Each scenario ($s \in S$) has a probability of occurrence (p^s). Therefore, Eq. (2) is reformulated to

$$E_{tjir}^{el} \leq \beta_j k_{ti} C_{tjir}^s + P_{tjir}^s \quad , \forall i \in I^{VRE}, j \in J, r \in R. \quad (3)$$

The included surplus variable P_{tjir}^s is associated with a real-world interpretation, which facilitates finding the penalty for it in the objective function. In Eq. (3), P_{tjir}^s describes the additional electricity that has to be purchased¹ by VRE technology i at time slice j of year t in region r under scenario s , in order to compensate the deviation from the optimal allocation of the independent system operator. As the additional electricity has to be purchased from external sources, a cost can be assigned to it in the objective function, thereby penalizing its occurrence. The objective function of the model minimizes the total system cost for different energy carriers and can be divided into a deterministic and a stochastic part,

$$z_t = \underbrace{\sum_i (z_{ti})}_{\text{deterministic term}} + \mathbb{E} \left[\underbrace{\sum_{ijs} (p_{ti}^{el} \cdot P_{tjir}^s)}_{\text{stochastic term}} \right] \quad , \forall t \in T. \quad (4)$$

The deterministic term includes, among other factors, the production, investment, and feedstock costs. The stochastic part, on the other hand, minimizes the expected (average) cost of purchasing additional electricity to satisfy the demand depending on the current power price (p_{ti}^{el}). It is assumed that any excess electricity production is wasted, as it will not be traded in the market.

We employ a combination of scenario and sensitivity analysis. The utilized scenarios ($s \in S$) are generated from the retrieved historical weather data, representing low, medium, and high values of cf to capture the variability in VRE availability and assess the system's response to extreme events. In each model run for each year t with a given probability ($Pr(S_c) \geq 0$), a scenario is picked according to Algorithm 1. Belongs the scenario to the low VRE availability scenario, the minimum possible cf is chosen for all time slices j in year t . For medium VRE availability, the average cf over all cf is computed and when the scenario belongs to a high VRE, the maximum cf is chosen. This process has to be repeated many times to obtain representative results, as each year may fall into these three categories under the given probability assumption. The stylized version of the code is presented in Algorithm 1.

Figure 2 shows the possible combination of scenarios in scenario space, which are picked over times. The sum of all probabilities is 100%. This figure builds the base for the ternary plots shown in the Result section III.

¹It happens in intraday and balancing markets.

Algorithm 1 Scenario generation algorithm

Require: $Pr(S_c) \geq 0$ such that $\sum_c Pr(S_c) = 1$

Require: x^{max} is the maximum number of replications

- 1: $x \leftarrow 0$
 - 2: **while** $x \leq x^{max}$ **do**
 - 3: $x \leftarrow x + 1$ \triangleright Generate multiple iterations
 - 4: $t \leftarrow 0$
 - 5: **while** $t \leq |T|$ **do**
 - 6: $t \leftarrow t + 1$
 - 7: $r \sim \mathcal{U}(0, 1)$ \triangleright Generate a random number between 0 and 1
 - 8: **if** $r \leq Pr(S_1)$ **then**
 - 9: $s_t^x = \min(s_t^x \in S_{c_1})$ \triangleright Choose scenario with the smallest capacity factor from S_{c_1}
 - 10: $p_x^s = p_x^s \times Pr(S_{c_1})$
 - 11: **else if** $r > Pr(S_{c_1})$ and $r \leq Pr(S_{c_1}) + Pr(S_{c_2})$ **then**
 - 12: $s_t^x = \mathbb{E}(S_{c_2})$ \triangleright Choose scenario with mean capacity factor from all scenarios in S_{c_2}
 - 13: $p_x^s = p_x^s \times Pr(S_{c_2})$
 - 14: **else**
 - 15: $s_t^x = \max(s_t^x \in S_{c_3})$ \triangleright Choose scenario with maximum capacity factor from S_{c_3}
 - 16: $p_x^s = p_x^s \times Pr(S_{c_3})$
 - 17: **end if**
 - 18: **end while**
 - 19: **end while**
 - 20: Run BENOPTex for the generated subset of scenarios (S^x, p_x^s)
-

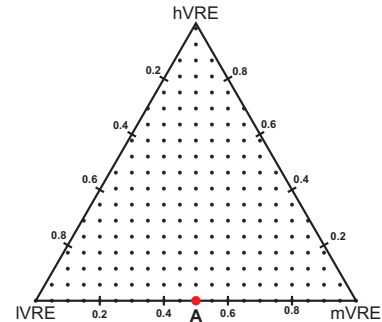


Fig. 2: All feasible combinations of scenarios in scenario space. Vertex A consists of 50% mVRE and 50% IVRE scenarios between 2020 and 2050.

The six-hourly stochastic model with $x^{max} = 100$ replications has been solved in 12 days with parallelization on a workstation with 72 Intel Xeon E-78867 processors at 2.4 GHz and 6 TB RAM. The GAMS optimizer is configured to assign six threads to CPLEX solvers: the primal and dual simplex algorithms have one thread each, and the interior point method has four threads [24]. Results are shown in section III.

III. RESULTS AND DISCUSSIONS

In this section, we present the results illustrating the interplay between VRE and bioenergy, depending on the selected scenario in the stochastic component of the model. The results are displayed as ternary plots in Figure 3. The triangular graphs represent the relationship between the three possible scenarios with each side of the triangle corresponding to the probabilities of one of the scenarios occurring. The intersection lines between the axes illustrate the dependencies among the scenarios. The results are not presented in absolute terms, but relative to the maximum value. Figure 3a shows the cost of the system. The color gradient reflects how different combinations of probabilities determine the total system cost. Point A represents the case where with 100% probability a value from the low-VRE scenario is chosen for each time slice of each year, point B indicates that always a value from the mid-VRE scenario is chosen; and point C denotes the case where with 100% probability a value from the high-VRE scenario is picked for each time slice of each year. The highest total system cost, shown in red, is reached when only low-VRE scenarios are picked. The system cost decrease as the probability of mid-VRE and high-VRE scenarios increase and reach the minimum value at point C. The distinctive line between the red and blue regions exhibits that if low-VRE conditions occur over 20% of the time until 2050, a dispatchable energy source (i.e., bioenergy) will be required to compensate for the imbalance between demand and supply cost-optimally. This result is confirmed in Figure 3b and Figure 3c. Figure 3b shows the amount of deployed VRE. It appears that the low-VRE scenario results in a limited proportion of VRE being utilized. Correspondingly, the bottom figure shows the amount of utilized bioenergy depending on the scenarios. When the probability of selecting a value from the mid-VRE scenario is high to very high, the amount of biomass used as an energy source decreases significantly.

In Figure 4, the amount of total energy production from biomass and VRE in Germany until 2050 is shown in EJ in comparison. The extreme Low-VRE setting corresponds to point (A) in the ternary plot, Mid-VRE corresponds to point (B), and High-VRE corresponds to point (C). Only biomass used for electricity production is considered in Figure 4. It is evident that bioenergy production decreases in both the Mid- and High-VRE scenarios. In contrast, solar PV production is consistently higher across all scenarios compared to bioenergy. Overall, the highest energy output is generated from onshore wind in the High-VRE scenario. It can also be observed that under the high-VRE setting, solar technology decreases unexpectedly. This behavior may be attributed to the nature of the optimal solution, where the dominant option—wind in this case—takes the entire share of renewables. In addition, a rise in total energy production across all considered technologies is detected. The total electricity production from 2020 until 2050 increases from 34.58 EJ in the Low-VRE scenario to 36.9 EJ in the Mid-VRE scenario, and reaches 39.9 EJ in the High-VRE scenario. Figure 5 shows the annual system costs

for three distinct scenarios, corresponding to points A, B, and C in Figure 3, until 2050. It is evident that the High-VRE scenario leads to the lowest system cost at every point in time while the extreme Low-VRE scenario results in the higher system cost. However, unlike the low-VRE setting, under the high-VRE scenario, steep growth in total system cost is visible. This growth is due to investments in solar and wind energy.

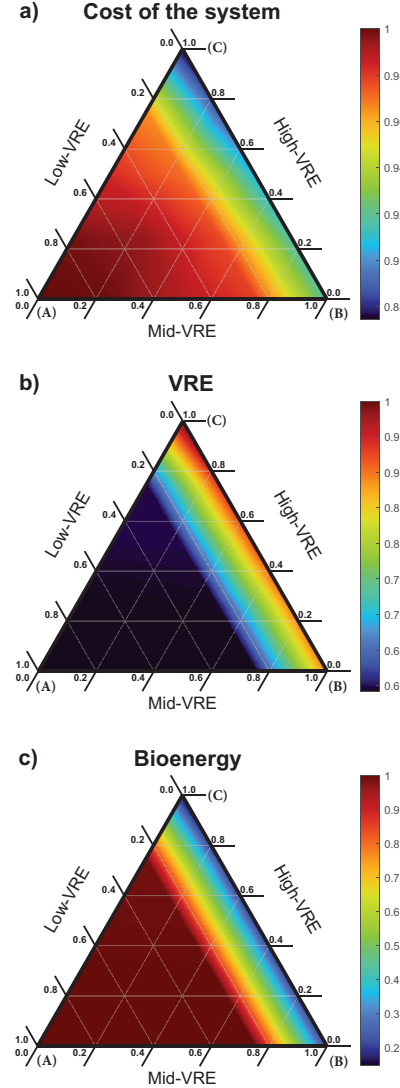


Fig. 3: The interplay between bioenergy and VRE with 6h time resolution and 100 replications for each setting.

IV. CONCLUSION

In conclusion, by integrating a stochastic component into our model, we captured the inherent variability and uncertainty of VRE. The results demonstrate that the fluctuating nature of VRE significantly influences the system cost, with scenarios characterized by a high share of VRE leading to lower system costs compared to scenarios with low VRE availability. This highlights the importance of accounting for VRE's variability in ESOMs, as higher VRE deployment, despite its fluctuations,

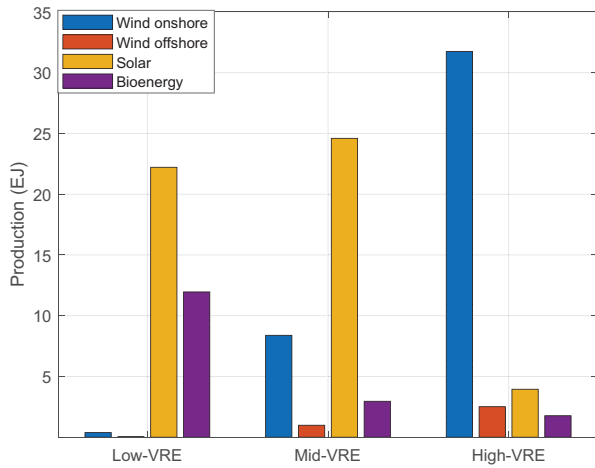


Fig. 4: Comparison of total bioenergy (electricity alone) and VRE production across different scenarios from 2020 to 2050. The Low-, Mid-, and High-VRE scenarios correspond to a 100% probability of selecting a capacity factor from the respective scenario.

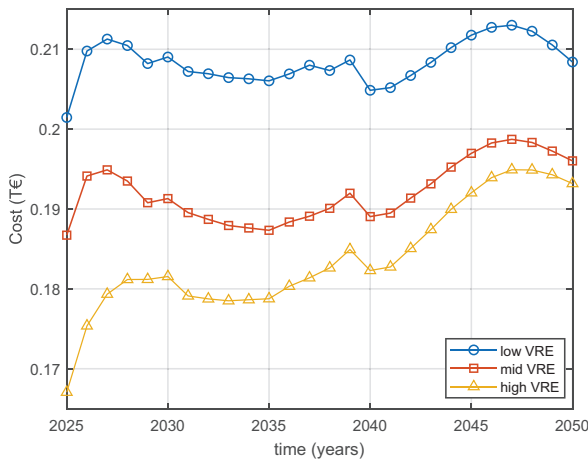


Fig. 5: Annual system costs in trillion Euros (10^{12}) for three different scenarios (Low-VRE in blue, Mid-VRE in red, High-VRE in yellow) from 2025 to 2050.

can lead to more cost-effective solutions in the long term. In situations with low VRE availability, bioenergy remains a necessary component of the energy mix, although its integration results in higher system costs. This highlights the importance of a balanced approach, where bioenergy can play a critical role in ensuring energy security when VRE availability is limited, but at a higher economic cost.

Comparing the production shows that the interplay between solar and onshore wind results in high investments in wind energy in the high-VRE scenario while in other cases solar PV is the dominating energy source. The next steps are to move from analyzing extreme scenarios to create scenarios with a probability distribution through clustering.

ACKNOWLEDGMENT

This study is funded by the *Man0EUvRE* (100695543), which is co-financed by means of taxation based on the budget adopted by the representatives of the Landtag of Saxony. ‘Man0EUvRE – Energy System Modelling for Transition to a net-Zero 2050 for EU via REPowerEU’ is funded by CETPartnership, the European Partnership under Joint Call 2022 for research proposals, co-funded by the European Commission (GA N°101069750).

REFERENCES

- [1] IEA, *Net Zero Roadmap: A Global Pathway to Keep the 1.5°C Goal in Reach*. IEA, Paris, 2023. [Online]. Available: <https://www.iea.org/reports/net-zero-roadmap-a-global-pathway-to-keep-the-15-0c-goal-in-reach>
- [2] B. H. Krepes, “The rising costs of fossil-fuel extraction: an energy crisis that will not go away,” *American Journal of Economics and Sociology*, vol. 79, no. 3, pp. 695–717, 2020.
- [3] E. Vartiainen, G. Masson, C. Breyer, D. Moser, and E. Román Medina, “Impact of weighted average cost of capital, capital expenditure, and other parameters on future utility-scale pv levelised cost of electricity,” *Progress in Photovoltaics: Research and Applications*, vol. 28, no. 6, pp. 439–453, 2020.
- [4] P. Denholm, D. J. Arent, S. F. Baldwin, D. E. Bilello, G. L. Brinkman, J. M. Cochran, W. J. Cole, B. Frew, V. Gevorgian, J. Heeter *et al.*, “The challenges of achieving a 100% renewable electricity system in the United States,” *Joule*, vol. 5, no. 6, pp. 1331–1352, 2021.
- [5] M. Lauer, M. Dotzauer, M. Millinger, K. Oehmichen, M. Jordan, J. Kalcher, S. Majer, and D. Thraen, “The crucial role of bioenergy in a climate-neutral energy system in germany,” *Chemical Engineering & Technology*, vol. 46, no. 3, pp. 501–510, 2023.
- [6] M. Sadr, D. Esmaili Aliabadi, B. Avşar, and D. Thrän, “Assessing the impact of seasonality on bioenergy production from energy crops in germany, considering just-in-time philosophy,” *Biofuels, Bioproducts and Biorefining*, 2024.
- [7] D. E. Aliabadi, M. Jordan, and D. Thrän, “The complementary role of utility-scale battery energy storage systems and bioenergy in future German transportation,” in *2023 19th International Conference on the European Energy Market (EEM)*. IEEE, 2023, pp. 1–6.
- [8] J. DeCarolis, H. Daly, P. Dodds, I. Keppo, F. Li, W. McDowall, S. Pye, N. Strachan, E. Trutnevtey, W. Usher *et al.*, “Formalizing best practice for energy system optimization modelling,” *Applied energy*, vol. 194, pp. 184–198, 2017.
- [9] S. Pfenninger, A. Hawkes, and J. Keirstead, “Energy systems modeling for twenty-first century energy challenges,” *Renewable and Sustainable Energy Reviews*, vol. 33, pp. 74–86, 2014.
- [10] P. Lopion, P. Markewitz, M. Robinius, and D. Stolten, “A review of current challenges and trends in energy systems modeling,” *Renewable and Sustainable Energy Reviews*, vol. 96, pp. 156–166, 2018.
- [11] T. Junne, M. Xiao, L. Xu, Z. Wang, P. Jochem, and T. Pregar, “How to assess the quality and transparency of energy scenarios: Results of a case study,” *Energy Strategy Reviews*, vol. 26, p. 100380, 2019.
- [12] G. Haydt, V. Leal, A. Pina, and C. A. Silva, “The relevance of the energy resource dynamics in the mid/long-term energy planning models,” *Renewable Energy*, vol. 36, no. 11, pp. 3068–3074, 2011.
- [13] S. Ludig, M. Haller, E. Schmid, and N. Bauer, “Fluctuating renewables in a long-term climate change mitigation strategy,” *Energy*, vol. 36, no. 11, pp. 6674–6685, 2011.
- [14] H. Maier, J. Guillaume, C. McPhail, S. Westra, J. Kwakkel, S. Razavi, H. van Delden, M. Thyer, S. Culley, and A. Jakeman, “Uncertainty, sensitivity and scenario analysis: how do they fit together?” 2021.
- [15] V. Gabrel, C. Murat, and A. Thiele, “Recent advances in robust optimization: An overview,” *European journal of operational research*, vol. 235, no. 3, pp. 471–483, 2014.
- [16] S. Bahramara and H. Golpiri, “Robust optimization of micro-grids operation problem in the presence of electric vehicles,” *Sustainable cities and society*, vol. 37, pp. 388–395, 2018.
- [17] D. L. McCollum, A. Gambhir, J. Rogelj, and C. Wilson, “Energy modellers should explore extremes more systematically in scenarios,” *Nature Energy*, vol. 5, no. 2, pp. 104–107, 2020.

- [18] M. Millinger, P. Tafarte, M. Jordan, F. Musonda, K. Chan, K. Meisel, and D. E. Aliabadi, "A model for cost- and greenhouse gas optimal material and energy allocation of biomass and hydrogen," *SoftwareX*, vol. 20, p. 101264, 2022.
- [19] S. Pfenninger and I. Staffell, "Long-term patterns of European PV output using 30 years of validated hourly reanalysis and satellite data," *Energy*, vol. 114, pp. 1251–1265, 2016.
- [20] I. Staffell and S. Pfenninger, "Using bias-corrected reanalysis to simulate current and future wind power output," *Energy*, vol. 114, pp. 1224–1239, 2016.
- [21] D. Esmaili Aliabadi, D. Manske, L. Seeger, R. Lehneis, and D. Thrän, "Integrating knowledge acquisition, visualization, and dissemination in energy system models: BENOPTex study," *Energies*, vol. 16, no. 13, p. 5113, 2023.
- [22] D. E. Aliabadi, K. Chan, N. Wulff, K. Meisel, M. Jordan, I. Österle, T. Pregger, and D. Thrän, "Future renewable energy targets in the EU: Impacts on the German transport," *Transportation Research Part D: Transport and Environment*, vol. 124, p. 103963, 2023.
- [23] N. Wulff, D. E. Aliabadi, S. Hasselwander, T. Pregger, H. C. Gils, S. Kronshage, W. Grimme, J. Horst, C. Hoyer-Klick, and P. Jochem, "Energy system implications of demand scenarios and supply strategies for renewable transportation fuels," *Energy Strategy Reviews*, vol. 58, p. 101606, 2025.
- [24] D. E. Aliabadi, K. Chan, M. Jordan, M. Millinger, and D. Thrän, "Abandoning the residual load duration curve and overcoming the computational challenge," in *2022 Open Source Modelling and Simulation of Energy Systems (OSMSES)*. IEEE, 2022, pp. 1–6.